

## Supporting Information

### **Periodicity in the Electrochemical Dissolution of Transition Metals**

*Florian D. Speck,\* Alexandra Zagalskaya, Vitaly Alexandrov, and Serhiy Cherevko\**

anie\_202100337\_sm\_miscellaneous\_information.pdf

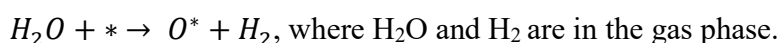
## Experimental Procedures

All polycrystalline metal working electrodes in this study (Fe, Co, Ni, Cu, as metal foils > 99.95% purity, and Ru, Rh, Pd, Ir, Pt, Au as metal disks, MaTeck, Germany; 99.9% purity<sup>1</sup>) were rigorously polished and rinsed thoroughly in ultra-pure water (18.2 M $\Omega$ , TOC < 5 ppb) before use. Afterward, a quick transfer to the SFC (scanning flow cell) setup was carried out to perform electrochemical measurements. The in-house developed SFC was contacted with a force of 500 mN during each experiment to gain an exposed electrode surface of 0.011 cm<sup>2</sup> reproducibly. The argon purged electrolyte was pumped to the ICP–MS (Perkin Elmer, NexION 350x) at a regularly calibrated flow rate of around 200  $\mu$ L min<sup>-1</sup>. The SFC setup featured an Ag/AgCl (Metrohm, 3 M KCl) reference electrode connected to the outgoing tube, a graphite rod in the electrolyte inlet tube was used as a counter electrode the above mentioned polycrystalline noble metals were set up as the working electrodes. All three electrodes were connected to a potentiostat (Gamry, Reference 600) controlled by a custom LabVIEW software. More details regarding the experimental setup and the online ICP-MS technique can be found in previous publications.<sup>2-3</sup> All potentials are referred to as V vs. the reversible hydrogen electrode (RHE) by regular calibration of the Ag/AgCl reference electrode in each electrolyte. The electrolytes were prepared from sodium hydroxide (99.99% Merck Suprapur®, 0.05 mol L<sup>-1</sup>), potassium hydroxide (99.99% Sigma-Aldrich Semiconductor grade, 0.05 mol L<sup>-1</sup>), or sulfuric acid (96% Merck Suprapur®, 0.1 mol L<sup>-1</sup>) by dilution with ultra-pure water. A uniform electrochemical procedure has been used to gather dissolution rates as well as total amounts. Here, a 300 s oxidation step, which, unless stated otherwise, was 200 mV over the first thermodynamic M/M<sup>n+</sup> transition. Physical material properties were extracted for stable bulk metal configurations from *The Materials Project* and correlated to the measured dissolution properties.<sup>4-5</sup>

Calibration of the ICP–MS was carried out daily for all investigated metals by a three-point calibration curve from freshly prepared standard solutions (Merck Centripur, 1 g L<sup>-1</sup> metal solutions in 2% HNO<sub>3</sub>). Furthermore, an internal standard was used to monitor the instrument's performance throughout the day. (<sup>57</sup>Fe, <sup>59</sup>Co, <sup>58</sup>Ni, <sup>63</sup>Cu using 20  $\mu$ g L<sup>-1</sup> of <sup>74</sup>Ge; <sup>102</sup>Ru using 10  $\mu$ g L<sup>-1</sup> of <sup>103</sup>Rh; <sup>103</sup>Rh using 10  $\mu$ g L<sup>-1</sup> of <sup>115</sup>In; <sup>106</sup>Pd using 50  $\mu$ g L<sup>-1</sup> of <sup>130</sup>Te; <sup>193</sup>Ir, <sup>195</sup>Pt, <sup>197</sup>Au using 10  $\mu$ g L<sup>-1</sup> of <sup>187</sup>Re). Finally, the last measurement of a standard solution at the end of the day to reproduce the calibration curve ensured the instrument's accuracy. The analyte signal was converted from counts into ng cm<sup>-2</sup> s<sup>-1</sup> using the calibration curve, the internal standards signal, the flow rate, and the electrode area.

## Theoretical values and descriptors

Binding energies  $\Delta E_O$  were taken from Ref.<sup>6</sup> where they were calculated for the most closed packed surfaces at a quarter of monolayer coverage. Generally, O binding energy is computed as:



Cohesive energies ( $\Delta E_{\text{coh}}$ ) were extracted from the Materials Project database<sup>4</sup> for the most stable bulk structures:

Metal (Materials Project ID)	Crystal system	$\Delta E_{\text{coh}}$ , eV
Au (mp-81)	cubic	2.99
Cu (mp-30)	cubic	3.50
Pd (mp-2)	cubic	3.70
Fe (mp-13)	cubic	5.05
Co (mp-54)	hexagonal	5.16
Pt (mp-126)	cubic	5.53
Rh (mp-74)	cubic	5.98
Ru (mp-33)	hexagonal	7.02
Ir (mp-101)	cubic	7.22

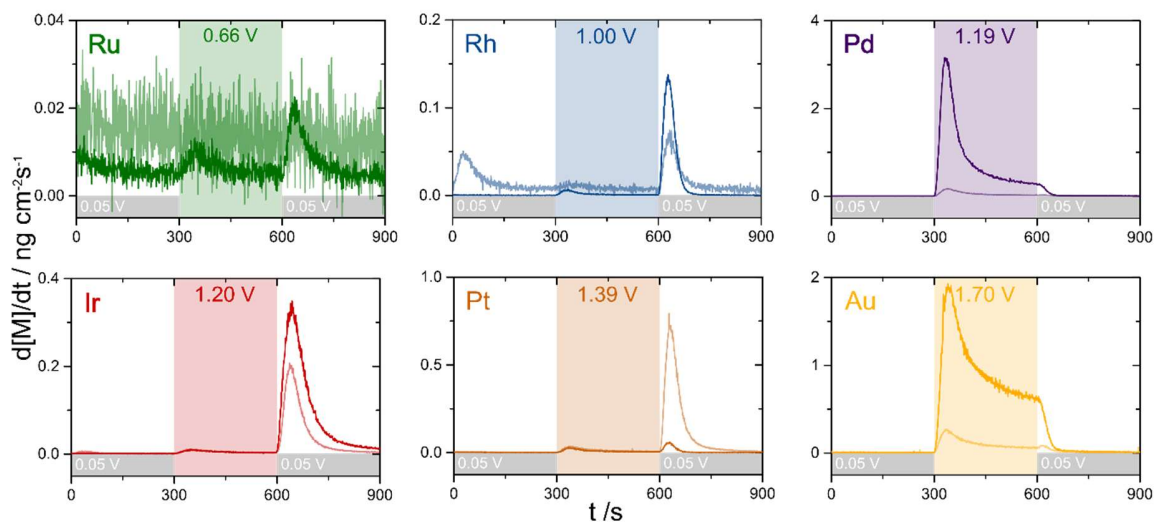


**Figure S1.** Comparison of dissolution rates for the investigated noble metals in the acidic (0.1 M  $\text{H}_2\text{SO}_4$ , solid line) and alkaline (0.05 M  $\text{NaOH}$ , pale line) electrolyte. After a reductive equalization of all metals during reduction at 0.05 V, a 200 mV oxidative step experiment was performed, followed by a second reductive step down to 0.05 V.

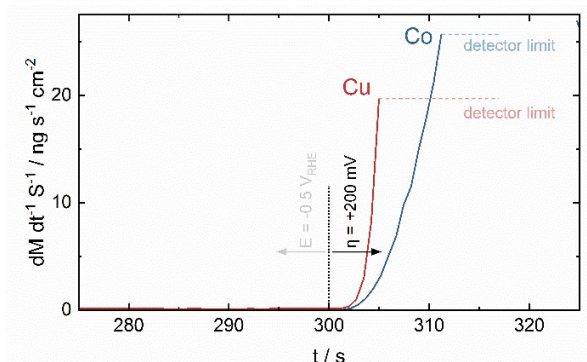


**Figure S2.** Example of 3d metal corrosion in an acidic (0.1 M H<sub>2</sub>SO<sub>4</sub>) electrolyte when stepping to an overpotential of 200 mV at t = 300 s.

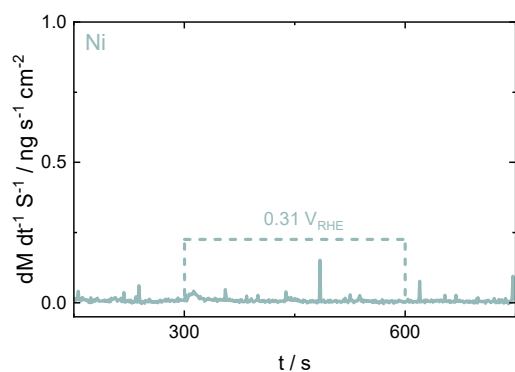


**Figure S3.** Ni dissolution during oxidation at 200 mV overpotential in an alkaline (0.05 M NaOH) environment.

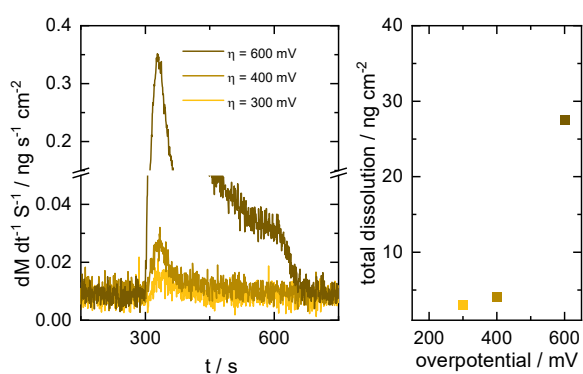


**Figure S4.** Dependence of anodic Ru dissolution in alkaline (0.05 M NaOH) on overpotential.

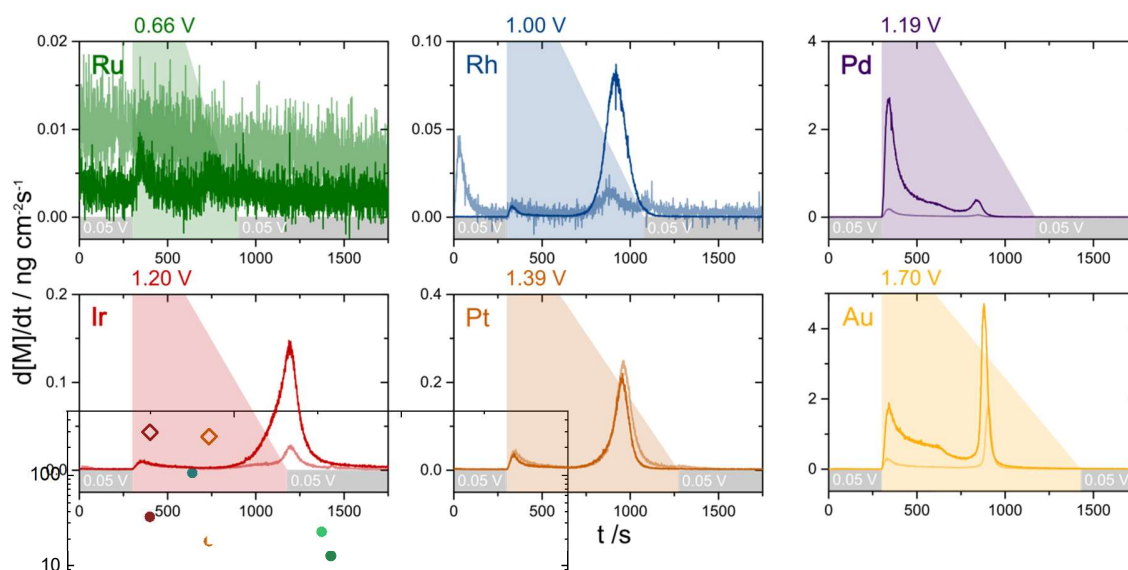


**Figure S5.** Dissolution rates of the investigated noble metals in acidic (0.1 M H<sub>2</sub>SO<sub>4</sub>, solid line) and alkaline (0.05 M NaOH, pale line) electrolyte. After a reductive equalization of all metals during reduction at 0.05 V, a 200 mV oxidative step experiment was performed. The oxidation was followed by a LSV at 2 mV s<sup>-1</sup> down to 0.05 V<sub>RHE</sub>.

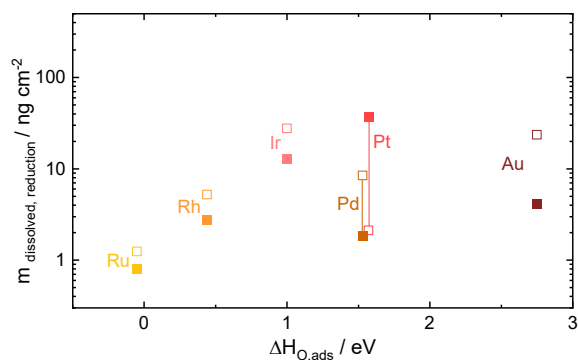


**Figure S6.** Dissolution associated with the reduction from Figure 2, plotted as a function of  $\Delta H_{O,ads}$ . (alkaline, 0.05 M NaOH: solid squares, acidic, 0.1 M H<sub>2</sub>SO<sub>4</sub>: hollow squares)

## References

- Schalenbach, M.; Kasian, O.; Ledendecker, M.; Speck, F. D.; Mingers, A. M.; Mayrhofer, K. J. J.; Cherevko, S., The Electrochemical Dissolution of Noble Metals in Alkaline Media. *Electrocatalysis* **2017**.
- Klemm, S. O.; Topalov, A. A.; Laska, C. A.; Mayrhofer, K. J. J., Coupling of a high throughput microelectrochemical cell with online multielemental trace analysis by ICP-MS. *Electrochem Commun.* **2011**, *13* (12), 1533-1535.

3. Topalov, A. A.; Katsounaros, I.; Meier, J. C.; Klemm, S. O.; Mayrhofer, K. J., Development and integration of a LabVIEW-based modular architecture for automated execution of electrochemical catalyst testing. *The Review of scientific instruments* **2011**, *82* (11), 114103.
4. Jain, A.; Ong, S. P.; Hautier, G.; Chen, W.; Richards, W. D.; Dacek, S.; Cholia, S.; Gunter, D.; Skinner, D.; Ceder, G.; Persson, K. A., The Materials Project: A materials genome approach to accelerating materials innovation. *APL Mater.* **2013**, *1* (1).
5. Ong, S. P.; Richards, W. D.; Jain, A.; Hautier, G.; Kocher, M.; Cholia, S.; Gunter, D.; Chevrier, V. L.; Persson, K. A.; Ceder, G., Python Materials Genomics (Pymatgen): A Robust, Open-source Python Library for Materials Analysis. *Comput. Mater. Sci.* **2013**, *68*, 314-319.
6. Nørskov, J. K.; Rossmeisl, J.; Logadottir, A.; Lindqvist, L.; Kitchin, J. R.; Bligaard, T.; Jónsson, H., Origin of the Overpotential for Oxygen Reduction at a Fuel-Cell Cathode. *J. Phys. Chem. B* **2004**, *108* (46), 17886-17892.